4880 Macromolecules 2002, 35, 4880−4887

New Titanium Complexes Bearing Two Indolide−Imine Chelate Ligands for the Polymerization of Ethylene

Tomoaki Matsugi, Shigekazu Matsui, Shin-ichi Kojoh, Yukihiro Takagi, Yoshihisa Inoue, Takashi Nakano, Terunori Fujita,* and Norio Kashiwa

R&D Center, Mitsui Chemicals, Inc., 580-32 Nagaura, Sodegaura-City, Chiba 299-0265, Japan

Received December 21, 2001; Revised Manuscript Received March 25, 2002

ABSTRACT: New titanium complexes **5**−**8** with two indolide−imine chelate ligands [7-(RN=CH)C_8H_5N]$_2$-$TiCl_2$ (R: **5**, phenyl; **6**, 2,6-difluorophenyl; **7**, 2,4,6-trifluorophenyl; **8**, pentafluorophenyl) were synthesized and investigated as ethylene polymerization catalysts. On activation with methylalumoxane (MAO), all of the complexes were active ethylene polymerization catalysts at 25 °C to produce linear polyethylenes. The catalytic activity (TOF) increased sharply with the number of fluorine atom in the ligand. In addition, complexes **5**−**8** potentially exhibit the characteristics of a living ethylene polymerization. Complexes **6** and **7** promoted room temperature living ethylene polymerization to produce polyethylenes having extremely narrow molecular weight distributions (**6**, M_w/M_n 1.09−1.14; **7**, M_w/M_n 1.05−1.23). On the other hand, at −10 °C complex **8** afforded monodisperse polyethylenes (M_w/M_n 1.12−1.25), with exceptionally high activities for a living ethylene polymerization (TOF: maximum 1155 min^{-1} atm^{-1}). Using complex **7**/MAO catalyst system, a polyethylene-*b*-poly(ethylene-*co*-propylene) block copolymer was successfully synthesized.

Introduction

During the past two decades, studies on single-site catalysts for olefin polymerization have been actively pursued in both academic and industrial research groups.[1−9] This is because single-site catalysts possess well-defined structures and, thus, provide a better opportunity for rational catalyst design than the heterogeneous Ziegler−Natta catalysts. The vast majority of the catalysts investigated are group 4 metallocene derivatives though some are known to involve one cyclopentadienyl (Cp) ligand. Therefore, recently, transition metal complexes with no Cp ligand(s) have received increased attention as potentially viable olefin polymerization catalysts. Recent progress in the rational design of well-defined transition metal complexes has resulted in the introduction of quite a few high-performance olefin polymerization catalysts, other than group 4 metallocene catalysts, based on both early and late transition metal complexes. Examples of high-performance catalysts feature chelating ligands such as diimine ligand (with Ni and Pd),[10] phenoxy−imine ligand (with Ni),[11] diimine−pyridine ligand (with Fe and Co),[12] amino−tropone ligand (with Ni),[13] diamide ligand (with Ti),[14] diamide−ether ligand (with Ti, Zr, Hf),[15] phosphine−imide ligand (with Ti),[16] pyrrolide−imine ligand (with Cr and Zr),[17] tris(pyrazolyl)borate ligand (with Ti),[18] bisphenoxy−amine ligand (with Zr),[19] and amide−pyridine ligand (with Ta).[20] Many of the complexes show activities comparable to those of group 4 metallocene catalysts and in some cases promote copolymerization of ethylene or α-olefins with polar olefins to produce functionalized polyolefins.[10b,11b] In addition, some function as living olefin polymerization catalysts to provide a variety of monodisperse polymers including polyolefinic block copolymers.[10c,14b,15a,19b,21−25] Consequently, the development of high-performance olefin polymerization catalysts has been achieved at a rapid pace.

Previously, in our laboratories, we have developed transition metal complexes featuring unsymmetrical bidentate ligands[26] [e.g., phenoxy−imine,[27,28] pyrrolide−imine,[29] imine−pyridine,[27e] and phenoxy−pyridine[30] ligands], which exhibit high catalytic performance for olefin polymerization including living olefin polymerization.[27h−j,l,n,29c] Further investigation along this research line has led to the discovery of titanium complexes bearing unsymmetrical bidentate indolide−imine chelate ligands, which display high ethylene polymerization activities and, moreover, can promote living ethylene polymerization to produce polyethylenes with extremely narrow molecular weight distributions.[31] Therefore, in this article, we describe the synthesis and ethylene polymerization behavior of a series of titanium complexes having two indolide−imine chelate ligands. In addition, we introduce the preparation of a polyethylene-*b*-poly(ethylene-*co*-propylene) block copolymer, and its evaluation results using transmission electron microscopy (TEM).

Results and Discussion

A general preparation route for titanium complexes utilized in this work is shown in Scheme 1. 7-Formylindole was synthesized according to the literature.[32]

The indolide−imine ligands **1**−**4**, 7-(*N*-aryliminomethyl)indole, are prepared in high yields (**1**, 98%; **2**, 64%; **3**, 72%; **4**, 70%) from the condensation of the appropriate aniline compound with 7-formylindole in toluene using acetic acid or *p*-toluenesulfonic acid as a catalyst. The titanium complexes **5**−**8** possessing two indolide−imine ligands, bis[7-(*N*-aryliminomethyl)indolinyl]titanium(IV) dichloride, are synthesized in moderate yields (**5**, 36%; **6**, 27%; **7**, 29%; **8**, 47%) in diethyl ether or toluene by treating $TiCl_4$ with 2 equiv of the lithium salt of the indolide−imine ligand.

The ^1H NMR spectra of titanium complexes **5**−**8** exhibit a single sharp peak assigned to the methine proton (−C=N−H) of the indolide−imine chelate ligand, being consistent with a six-coordinate octahedral structure. The titanium complexes could exhibit five idealized octahedral isomeric structures A−E (Scheme 2) because

10.1021/ma0122268 CCC: $22.00

Scheme 1

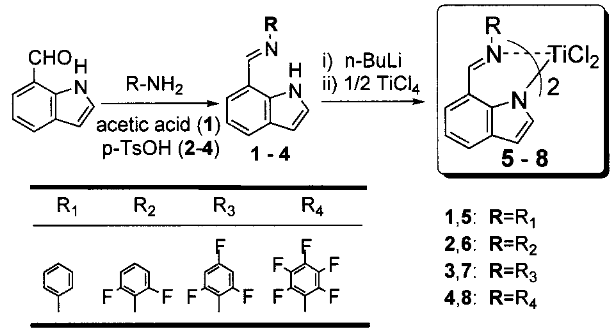

Scheme 2

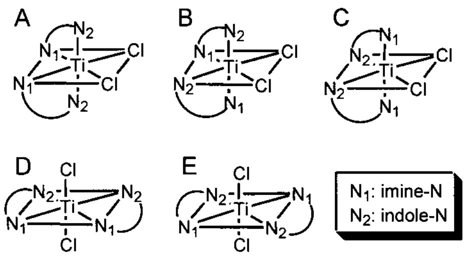

they possess two unsymmetrical bidentate ligands. Thus, the complexes potentially have more than one active species for olefin polymerization.

Since, as reported,[27e,29] DFT calculations are an effective tool for analyzing the structures of group 4 transition metal complexes, DFT calculations were performed on a methyl cationic complex, an initial active species generated from complex **5** with MAO for ethylene polymerization, to obtain information on the structure of an active species. The cationic complex was suggested to possess a distorted octahedral coordination structure around the titanium metal, an isomer-A-type structure, in which a methyl group and a coordinated ethylene are situated at an angle of 63.9° (Figure 1), showing that for ethylene polymerization the cationic complex has a pair of available cis-located sites, which are trans to the imine nitrogens in the ligand. Likewise, the calculations indicated that the methyl cationic complexes originated from complexes **6**−**8** also adopt an isomer-A-type structure (methyl-Ti-coordinated ethylene angle; **6**, 70.4°; **7**, 71.2°; **8**, 74.4°). Therefore, complexes **5**−**8** were suggested to possess two available cis-located sites, a prerequisite for efficient olefin polymerization, and at the same time, the same stereochemical relationship between the active sites and the imine nitrogens as the previously reported group 4 transition metal complexes with phenoxy−imine or pyrrolide−imine chelate ligands, which display high ethylene polymerization activities.

Ethylene Polymerization Behavior of Complexes 5−8/MAO Catalyst Systems. Complexes **5**−**8** were investigated for their potential as ethylene polymerization catalysts at 25 °C under atmospheric pressure using methylalumoxane (MAO) as a cocatalyst. The results are summarized in Table 1. All of the complexes are active ethylene polymerization catalysts to produce crystalline polyethylenes. The activities (TOF) obtained were in the range of 31−677 min^{-1} atm^{-1}. The basic trend observed regarding catalytic activity is that increase in the number of fluorine atoms in the ligand resulted in enhanced catalytic activity (e.g., complex **8** is over 20 times more active than the corresponding nonfluorinated complex **5**). These results provide a clear demonstration that the electrophilicity of the titanium center in active species plays a dominant role in determining the catalytic activity, unlike the group 4 metallocene catalysts whose activity is decreased by the introduction of electron-withdrawing substituent(s) in Cp ligand.[33,34] An explanation for the activity enhancement resulting from the introduction of electron-withdrawing fluorine atom(s) in the ligand is that a more electrophilic titanium center, generated by a more electron-withdrawing ligand, results in increase metal−carbon reactivity, leading to reduced activation energy for ethylene insertion. The activity, TOF 677 min^{-1} atm^{-1}, exhibited by complex **8** is very high for a titanium complex with no Cp ligand(s) and is comparable to that displayed by the highly active titanium complex with two phosphinimide ligands reported by Stephan et al.[16] (TOF 693 min^{-1} atm^{-1}, 25 °C, atmospheric pressure).

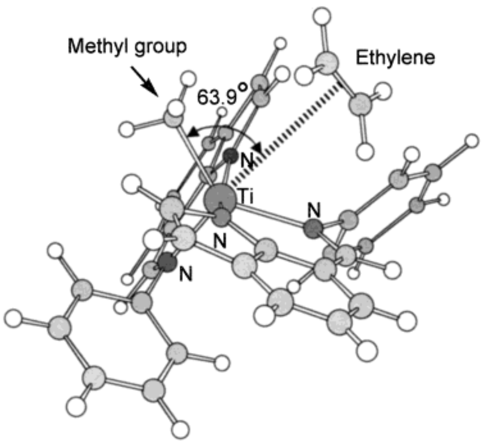

Figure 1. Calculated structure of ethylene coordinated active species generated from complex **5**.

Table 1. Ethylene Polymerization Results Using Complexes 5−8[a]

entry	complex	yield (g)	TOF[b] (min^{-1} atm^{-1})	M_w[c] (10^{-4})	M_w/M_n[c]
1	**5**	0.043	31	1.38	1.14
2	**6**	0.050	36	1.24	1.13
3	**7**	0.240	171	4.65	1.11
4	**8**	0.951	677	32.3	1.93

[a] Conditions: 25 °C, 0.1 MPa pressure, polymerization time; 10 min, ethylene 100 L/h, complex; 5.0 μmol; cocatalyst MAO (Al) 1.25 mmol, solvent; toluene 250 mL. [b] TOF: [polymer yield (g)]/28.05/[complex (mol)]/[polymerization time (min)]. [c] M_w, M_n values; GPC analysis.

Complexes **5**−**8** provided polyethylenes having moderate to high molecular weight values (M_w 13 800−323 000). The polyethylenes exhibit the peak melting temperature (T_m) in the range 132.2−134.2 °C. ^{13}C NMR analyses indicate that the polyethylenes possess linear structures with virtually no branching. Analyses of the polyethylene end groups by ^{13}C NMR as well as IR show that the polyethylenes are essentially saturated, indicating that β-hydride elimination is negligible as a chain termination process concerning complexes **5**−**8**/MAO catalyst systems. GPC analyses of the polymers revealed that the polyethylenes produced by complexes **5**−**7** possess extremely narrow molecular weight distributions (M_w/M_n 1.11−1.14) whereas that formed with complex **8** has an M_w/M_n value of 1.93. The M_w/M_n values suggest that complexes **5**−**7**/MAO catalyst sys-

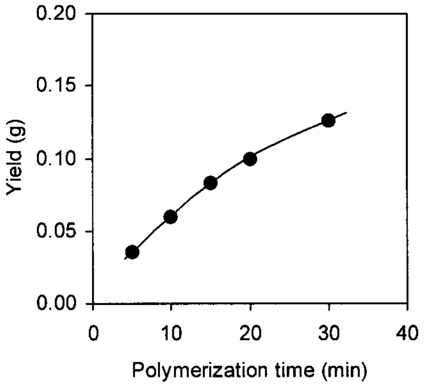

Figure 2. Plot of polymer yield as a function of polymerization time for the polymerization of ethylene using complex **5**/MAO (25 °C).

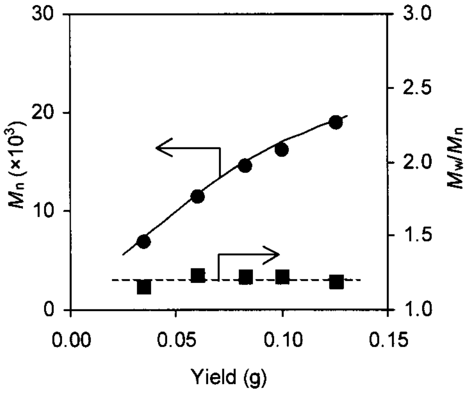

Figure 3. Plot of M_n and M_w/M_n as a function of polymer yield for the polymerization of ethylene using complex **5**/MAO (25 °C).

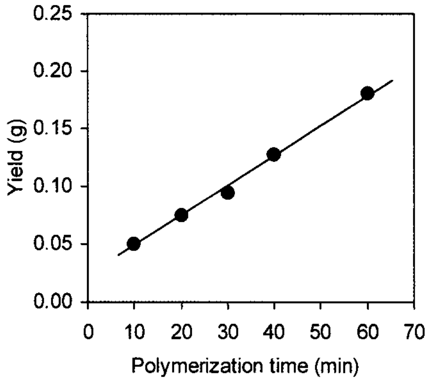

Figure 4. Plot of polymer yield as a function of polymerization time for the polymerization of ethylene using complex **6**/MAO (25 °C).

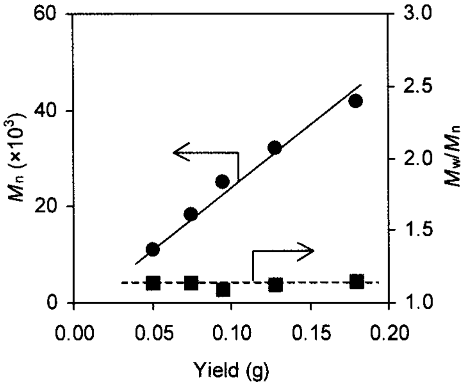

Figure 5. Plot of M_n and M_w/M_n as a function of polymer yield for the polymerization of ethylene using complex **6**/MAO (25 °C).

tems may have the characteristics of a living ethylene polymerization under the given conditions despite the use of MAO, a potential chain transfer agent, as the cocatalyst.

Detailed Study on Ethylene Polymerization Behavior of Complexes 5−8/MAO. Ethylene polymerizations using complex **5**−**8**/MAO were further investigated to elucidate the catalytic performance of complexes **5**−**8**/MAO catalyst systems.

Complex 5/MAO Catalyst System. The polymer yield−polymerization time and M_n and M_w/M_n values−polymer yield relationships were plotted for the polymerization with complex **5**/MAO catalyst system at 25 °C under ethylene at atmospheric pressure (Figures 2 and 3). As shown in Figure 2, an increase of polymer yield against polymerization time showed gradual saturation behavior despite the sufficiently low polymer yields and M_n values of the polyethylenes, indicating that some catalyst deactivation occurred during the polymerization. However, the M_n value increased proportionally with the polymer yield, and the narrow M_w/M_n value was retained during the course of the polymerization (Figure 3). These results suggest that complex **5**/MAO catalyst system possesses the considerable characteristics of living ethylene polymerization at room temperature though some catalyst deactivation is observed under the given conditions.

Complexes 6 and 7/MAO Catalyst Systems. Figure 4 shows the plot of polymer yield as a function of polymerization time with respect to the polymerization of ethylene using complex **6**/MAO catalyst system. The polymer yield increased linearly with the polymerization time, indicating that the catalyst deactivation was negligible under the conditions employed. The plots of M_n and M_w/M_n vs polymer yield are shown in Figure 5. A linear relationship between M_n and the polymer yield as well as narrow M_w/M_n values for all runs (M_w/M_n 1.05−1.23) were found (Figure 5). Likewise, linear relationships vis-à-vis the polymer yield vs polymerization time and M_n and M_w/M_n values vs polymer yield were found for complex **7**/MAO catalyst system (see the Supporting Information). These results indicate that complexes **6** and **7**/MAO catalyst systems promote the living polymerization of ethylene at 25 °C. These are rare examples of room temperature living ethylene polymerizations. Considering that the MAO used as the cocatalyst is a potential chain transfer agent, the room temperature living ethylene polymerizations exhibited by complexes **6** and **7** are highly significant. The activities, TOF 124−188 min^{-1} atm^{-1}, displayed by complex **7** are very high for a polymerization proceeding in a living fashion. As listed in Table 2, at 50 °C complex **7** was capable of producing polyethylene having reasonably narrow molecular weight distribution (M_w/M_n 1.24) though at 75 °C the complex furnished polyethylene with broad molecular weight distribution (M_w/M_n 15.9) probably due to considerable catalyst deactivation.

Complex 8/MAO Catalyst System. The plot of polymer yield vs polymerization time and the plot of M_n and M_w/M_n vs polymer yield are shown in Figures 6 and 7.

Although an increase of polymer yield vs the polymerization time and that of M_n vs polymer yield showed gradual saturation behavior, the produced polymer

Table 2. Ethylene Polymerization Results with Complex 7/MAO Catalyst System[a]

entry	temp (°C)	yield (g)	TOF[b] (min^{-1} atm^{-1})	M_w[c] (10^{-4})	M_w/M_n[c]
1	25	0.240	171	4.65	1.11
2	50	0.242	173	6.61	1.24
3	75	0.063	44.9	31.2	15.9

[a] Conditions: 0.1 MPa pressure, polymerization time; 10 min, ethylene 100 L/h, complex **7**; 5.0 μmol; cocatalyst MAO (Al) 1.25 mmol, solvent; toluene 250 mL. [b] TOF: [polymer yield (g)]/28.05/[complex (mol)]/[polymerization time (min)]. [c] M_w, M_n values; GPC analysis.

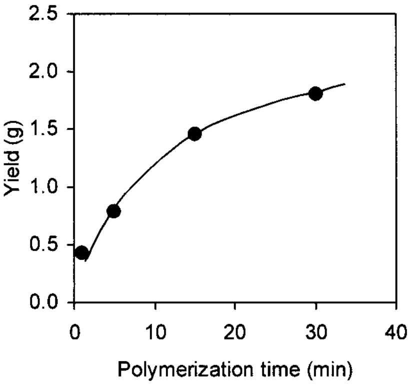

Figure 6. Plot of polymer yield as a function of polymerization time for the polymerization of ethylene using complex **8**/MAO (25 °C).

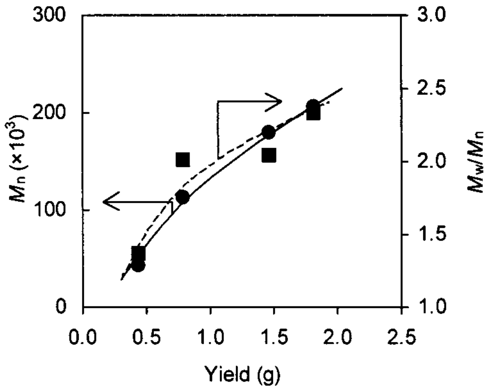

Figure 7. Plot of M_n and M_w/M_n as a function of polymer yield for the polymerization of ethylene using complex **8**/MAO (25 °C).

chain number, calculated from the polymer yield and M_n value, suggested that each molecule of catalyst makes approximately one polymer chain. IR analyses showed that the polyethylenes formed with complex **8** possess essentially saturated end groups. In addition, changing the Al/Ti ratio gave rise to practically no changes in molecular weight. These results show that the polymerization process is not only devoid of chain termination via β-hydride elimination, but also it proceeds without chain transfer to the aluminum cocatalyst though some catalyst deactivation may be involved in the process. The increase in M_w/M_n value during the course of polymerization results mainly from the inhomogeneity of the polymerization system because of high molecular weight and insoluble polymers. As listed in Table 3, hydrogen works as an effective chain transfer agent in the polymerization of ethylene with complex **8** to give lower molecular weight polyethylenes with increased number of polymer chains per catalyst molecule.

Table 3. Effects of MAO or H_2 on Ethylene Polymerization Behavior of Complex 8/MAO Catalyst System[a]

entry	MAO (mmol)	H_2 feed (L/h)	yield (g)	TOF[b] (min^{-1} atm^{-1})	M_w[c] (10^{-4})	M_w/M_n[c]	[N][d]
1	0.5	0	0.41	290	40.0	3.06	0.62
2	1.25	0	0.79	563	40.2	2.84	1.12
3	2.5	0	0.97	689	42.0	2.29	1.05
4	5.0	0	1.19	848	40.5	2.09	1.23
5	12.5	0	1.42	1013	43.8	1.97	1.28
6	2.5	5	0.64	459	1.96	1.79	11.7
7	2.5	10	0.50	358	1.25	2.04	16.5

[a] Conditions: 25 °C, 0.1 MPa pressure, polymerization time; 10 min, toluene; 250 mL, ethylene; 100 L/h, complex **8**; 5.0 μmol. [b] TOF: [polymer yield (g)]/28.05/[complex (mol)]/[polymerization time (min)]. [c] M_w, M_n values; GPC analysis. [d] [N] = number of polymer chains (mol [PE]/mol [cat.]).

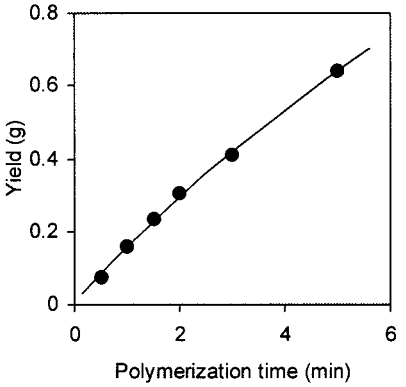

Figure 8. Plot of polymer yield as a function of polymerization time for the polymerization of ethylene using complex **8**/MAO (−10 °C).

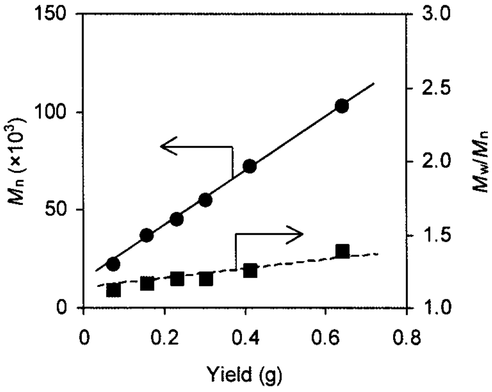

Figure 9. Plot of M_n and M_w/M_n as a function of polymer yield for the polymerization of ethylene using complex **8**/MAO (−10 °C).

Ethylene polymerizations using complex **8**/MAO were carried out at a lower temperature of −10 °C and at a lower catalyst concentration. The polymer yield−polymerization time and M_n and M_w/M_n values−polymer yield relationships are plotted (Figures 8 and 9).

The M_n value increased proportionally with the polymerization time, and at the same time, the narrow M_w/M_n value was retained during the polymerization (M_w/M_n 1.12−1.25), indicating that complex **8**/MAO promotes living ethylene polymerization at −10 °C. It is noteworthy that the activities exhibited by complex **8**/MAO, TOF 979−1155 min^{-1} atm^{-1}, are 2 orders of magnitude greater than those obtained with common living ethylene polymerization systems (TOF ca. 20

Table 4. Preparation of PE-*b*-poly(ethylene-*co*-propylene) and Its Segments[a]

entry	time (min)	monomer	yield (g)	M_n[a] (10^{-4})	M_w/M_n[a]	P[b] (mol %)
1[c]	5−50	E to E/P	0.45	3.14	1.17	8.0
2	5	E	0.16	1.52	1.05	0
3	50	E/P	0.38	2.41	1.22	19.5

[a] Conditions: 2.0 °C, 0.1 MPa pressure, complex **7**; 10 μmol, MAO(Al) 2.50 mmol (Al). Toluene (250 mL) saturated with ethylene employed as a solvent. [b] M_w, M_n values; GPC analysis. [c] Total propylene contents in the resulting polymers; IR analysis. [d] After ethylene (100 L/h, 5 min) polymerization, the feeding gas was changed from ethylene to mixed gas (ethylene/propylene = 30/70 L/h, 50 min).

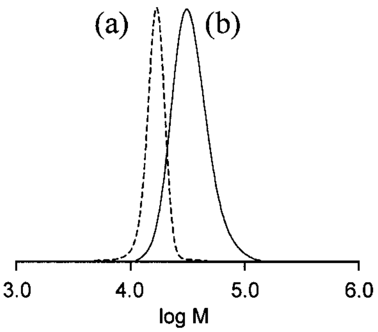

Figure 10. GPC traces of the polymers: (a) polyethylene (Table 4, entry 2); (b) PE-*b*-poly(ethylene-*co*-propylene) (Table 4, entry 1).

min^{-1} atm^{-1}). Moreover, these activities represent some of the highest activities reported to date for titanium-based ethylene polymerization catalysts with no Cp ligands at atmospheric pressure conditions.

Although the catalytic activity shows a marked dependency on the number of fluorine atoms in the ligand with respect to the complexes used in this study, complex **5** having no fluorine in the ligand inserts ethylene in a living fashion. Therefore, the realization of the living polymerization by the complexes is probably ascribed to the bulky and rigid indolide−imine ligands, which suppress chain termination or transfer steps, unlike titanium complexes having fluorine-containing phenoxy−imine ligands in which the presence of fluorine(s) is a requirement for living polymerization.

Synthesis of PE-*b*-poly(ethylene-*co*-propylene) Block Copolymer Using Complex 7/MAO Catalyst System. The usefulness of living olefin polymerization catalysts is largely proportional to their potential for preparing polyolefinic block copolymers, which may be applied to a broad spectrum of areas including compatibilizers, elastomers, and composite materials. Thus, we decided to synthesize a well-defined polyethylene-*b*-poly(ethylene-*co*-propylene) A−B diblock copolymer comprised of crystalline and amorphous segments in order to show the usefulness of the catalyst system. Treatment of complex **7** (10.0 μmol)/MAO (2.50 mmol) catalyst system with ethylene (100 L/h) for 5 min and then with ethylene−propylene (ethylene, 30 L/h; propylene, 70 L/h) for 50 min at 2 °C resulted in the formation of a well-defined high molecular weight PE-*b*-poly(ethylene-*co*-propylene) block copolymer having extremely narrow polydispersity. An overlay of the unimodal GPC elution curves for the PE A block (M_n 15 200, M_w/M_n 1.05) and the final PE-*b*-poly(ethylene-*co*-propylene) A−B diblock (M_n 31 400, M_w/M_n 1.17) indicates a shift toward higher molecular weight region due to the subsequent copolymerization step without providing any peak in the low-molecular-weight region (Figure 10), demonstrating the creation of the target block copolymer. The poly(ethylene-*co*-propylene) segment of the block copolymer is estimated to contain 19.5 mol % of propylene, based on the control experiment (Table 4, entry 3). The peak melting temperature (T_m) of the resulting block polymer and the corresponding PE homopolymer were determined from DSC measurements. The PE-*b*-poly(ethylene-*co*-propylene) displays a lower T_m, 126.8 °C, relative to that of the PE homopolymer (134.1 °C, entry 2). The decrease in T_m vis-à-vis the block copolymer is probably due to the fact that the crystalline state is disturbed by the segregation process of incompatible components consisting of crystalline PE and amorphous poly(ethylene-*co*-propylene) segments which are chemically linked, further confirming the formation of the block copolymer. This is a rare example of the synthesis of ethylene-based polyolefinic block copolymer consisting of crystalline and amorphous segments.[27h,i] Further information on the properties of the block copolymer is provided by transmission electron microscopy (TEM). TEM was applied to study the morphology difference between the PE-*b*-poly(ethylene-*co*-propylene) and the corresponding PE/poly(ethylene-*co*-propylene) blend polymer (blend conditions; toluene, reflux temperature, 1 h). The TEM image of the block copolymer is quite different from that of the blend polymer as can be seen in Figure 11. Thus, the TEM micrograph of the press sheet made of the block copolymer shows well-defined morphology of microphase separation. In Figure 11A, white domains corresponding to the PE segment form a fine nanostructure, whereas those for the blend polymer (Figure 11B) display the grown lamellar structures of PE, and the poly(ethylene-*co*-propylene) exists among the PE lamellar structures. These results indicate that the block copolymer has a high potential as a compatibilizer.

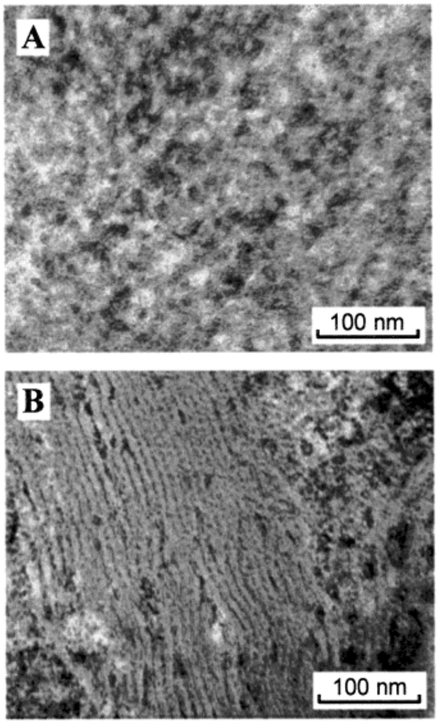

Figure 11. TEM micrographs of (A) PE-*b*-poly(ethylene-*co*-propylene) and (B) polyethylene and poly(ethylene-*co*-propylene) blend polymer (blend conditions; toluene, reflux temperature, 1 h).

Conclusion

In conclusion, a series of titanium complexes **5**−**8** featuring a pair of indolide−imine chelate ligands have been introduced, which possess high catalytic performance for the polymerization of ethylene using MAO as a cocatalyst. Complexes **5**−**8** can polymerize ethylene in a living fashion to form linear polyethylenes. Thus, complexes **6** and **7** conduct room temperature living ethylene polymerization to provide polyethylenes with extremely narrow molecular weight distributions. In addition, complex **8** having pentafluorophenyl in the ligand at −10 °C promote high-speed living ethylene polymerization to produce monodisperse polyethylenes with high molecular weight values. The catalytic activities displayed by complex **8** are 2 orders of magnitude larger than those of common living ethylene polymerization catalysts. Moreover, with complex **7**/MAO catalyst system, a PE-*b*-poly(ethylene-*co*-propylene) block copolymer has been successfully prepared, which may be useful as a compatibilizer. Therefore, the titanium complexes described herein represent a notable addition to the limited list of high-performance titanium complexes with no Cp ligands for olefin polymerization.

Experimental Section

General Procedures and Materials. All manipulations of air- and/or water-sensitive materials were carried out under a dry nitrogen atmosphere using standard Schlenk cannula techniques or in a conventional nitrogen-filled glovebox.

Dried solvents (diethyl ether, ethanol, dichloromethane (CH_2Cl_2), *n*-hexane, *n*-pentane, and toluene) used for ligand and complex syntheses were purchased from Wako Pure Chemical Industries, Ltd., and used without further purification. 7-Formylindole was prepared according to an established procedure. $TiCl_4$ was purchased from Aldrich Chemical Co., Inc. Ethylene was obtained from Sumitomo Seika Co., Ltd. Methylalumoxane (MAO) was purchased from Albemarle as a 1.2 M toluene solution, and the remaining trimethylaluminum was evaporated in vacuo prior to use. Toluene used as a polymerization solvent (Wako Pure Chemical Industries, Ltd.) was dried over Al_2O_3. All other chemicals were obtained commercially and used as received.

Ligand and Complex Analyses. ^1H NMR spectra were recorded on a JEOL 270 spectrometer (270 MHz) in $CDCl_3$ with tetramethylsilane as the internal standard at ambient probe temperature (25 °C). Chemical shifts were reported in δ units. The melting point (mp) of a ligand was measued by a melting point microapparatus from Yanagimoto Seisakusho. FD-MS spectra were recorded on an SX-102A from Japan Electron Optics Laboratory Co., Ltd. Elemental analysis for CHN was performed by a CHNO type from Helaus Co.

Polymer Analyses. ^{13}C NMR spectra for polyethylene were recorded on an NEC-LA500 spectrometer (125 MHz) using *o*-dichlorobenzene with 20% benzene-d_6 as a solvent at 120 °C. Molecular weight distribution (M_w/M_n) values of polymers were determined using a Waters 150-C gel permeation chromatograph at 145 °C using polyethylene calibration and equipped with three TSKgel columns (two sets of TSKgelGMH$_{HR}$-H(S)-HT and TSKgelGMH$_6$-HTL). *o*-Dichlorobenzene was used as a solvent at a flow rate of 1.0 mL/min. Vinyl end group concentration of the polyethylenes and propylene contents of the copolymers were determined by IR analyses using FT/IR-350 from JASCO Co. Peak melting temperatures (T_m) of the polymers were determined by DSC with a Shimazu DSC-60 differential scanning calorimeter, measured upon reheating the polymer sample to 200 °C at a heating rate of 10 °C/min. Transmission electron microscopy (TEM) images were obtained using a HITACHI H-8100 transmission electron microscopy.

Complex Syntheses. 7-(PhNCH)C_8H_5NH (1). Acetic acid (0.3 mL) was added to a stirred solution of 7-formylindole (1.20 g, 8.27 mmol) and aniline (0.77 g, 8.27 mmol) in ethanol (40 mL) at room temperature. The mixture was stirred for 3 h at room temperature and then concentrated in vacuo to afford **1** (1.78 g, 8.10 mmol) as yellow oil in 98% yield. ^1H NMR (270 MHz, $CDCl_3$): δ. 6.55 (dd, 1H, indole ring aromatic H), 7.1−7.4 (m, 6H, indole ring aromatic H and benzene ring aromatic H), 7.73 (d, 1H, indole ring aromatic H), 8.63 (s, 1H, CH═N), 10.76 (bs, 1H, NH). ^{13}C NMR (100 MHz, $CDCl_3$): 102.4, 119.3, 119.4, 120.9, 124.6, 125.1, 125.8, 126.6, 128.5, 129.3, 133.8, 151.9, 161.3. FD-MS (*m*/*z*) 220 (M^+).

7-(2,3,4,5,6-F(Ph)NCH)C_8H_5NH (4). *p*-Toluenesulfonic acid monohydrate (20 mg) was added to a stirred solution of 7-formylindole (1.60 g, 11.0 mmol) and pentafluoroaniline (2.11 g, 11.5 mmol) in dried toluene (50 mL) at room temperature. The mixture was stirred for 2 h at 40 °C, and then the toluene was evaporated in vacuo at 40 °C to give a residue. The residue was dissolved in dried toluene (50 mL) and stirred for 1 h at 40 °C. The toluene was evaporated in vacuo to give a solid residue. To the residue, dichloromethane (15 mL) and hexane (30 mL) were added, and the resulting mixture was filtered through a glass filter. The filtrate was concentrated in vacuo to give a solid. Recrystallization from dried ethyl acetate (5 mL) and *n*-hexane (30 mL) yielded **4** (2.39 g, 7.70 mmol) as a pale yellow solid in 70% yield; mp 157 °C. ^1H NMR (270 MHz, $CDCl_3$): δ. 6.66 (dd, 1H, indole ring aromatic H), 7.23 (m, 1H, indole ring aromatic H), 7.39 (dd, 1H, indole ring aromatic H), 7.48 (dd, 1H, indole ring aromatic H), 7.89 (d, 1H, $J = 7.6$ Hz, indole ring aromatic H), 8.88 (m, 1H, CH═N), 10.58 (bs, 1H, NH). ^{13}C NMR (100 MHz, $CDCl_3$): 102.7, 118.7, 119.4, 125.5, 126.1, 126.5, 128.0, 128.9, 133.7, 136.8−136.9, 139.0−139.5, 141.6−141.8, 141.7, 169.0. $C_{15}H_7N_2F_5$ 310.23. Calcd: C, 58.08; H, 2.27; N, 9.03. Found: C, 58.10; H, 2.30; N, 8.91. FD-MS (*m*/*z*) 310 (M^+).

7-(2,6-F(Ph)NCH)C_8H_5NH (2). **2** was prepared using a procedure similar to that for **4**; mp 119 °C. ^1H NMR (270 MHz, $CDCl_3$): δ. 6.64 (dd, 1H, indole ring aromatic H), 6.95−7.12 (m, 3H, benzene ring aromatic H), 7.24 (t, 1H, indole ring aromatic H), 7.38 (dd, 1H, indole ring aromatic H), 7.47 (dd, 1H, indole ring aromatic H), 7.84 (d, 1H, $J = 8.1$ Hz, indole ring aromatic H), 8.92 (m, 1H, CH═N), 10.80 (bs, 1H, NH). ^{13}C NMR (100 MHz, $CDCl_3$): 102.4, 111.7−112.0, 119.2, 119.4, 125.1−125.3, 125.4, 125.5, 127.3, 128.1−128.3, 128.7, 133.7, 154.3−156.8, 167.2. FD-MS (*m*/*z*) 256 (M^+).

7-(2,4,6-F(Ph)NCH)C_8H_5NH (3). **3** was prepared using a procedure similar to that for **4**; mp 103 °C. ^1H NMR ($CDCl_3$): δ. 6.64 (dd, 1H, indole ring aromatic H), 6.73−6.87 (m, 2H, benzene ring aromatic H), 7.22 (t, 1H, indole ring aromatic H), 7.38 (dd, 1H, indole ring aromatic H), 7.45 (dd, 1H, indole ring aromatic H), 7.84 (d, 1H, $J = 7.8$ Hz, indole ring aromatic H), 8.91 (m, 1H, CH═N), 10.70 (bs, 1H, NH). ^{13}C NMR (100 MHz, $CDCl_3$): 100.4−101.0, 102.4, 119.3, 119.4, 124.8−125.0, 125.1, 125.5, 127.3, 128.7, 133.7, 154.3−157.0, 157.5−160.3, 167.0. FD-MS (*m*/*z*) 274 (M^+).

[7-(PhNCH)C_8H_5N]$_2$$TiCl_2$(5). To a stirred solution of **1** (0.85 g, 3.86 mmol) in dried diethyl ether (15 mL) at −78 °C, a 1.56 M *n*-butyllithium hexane solution (2.50 mL, 3.90 mmol) was added dropwise over a 15 min period. The mixture was allowed to warm to room temperature and stirred for 4 h. The resulting solution was added dropwise over a 20 min period to a 0.5 M *n*-heptane solution of $TiCl_4$ (3.86 mL, 1.93 mmol) in dried diethyl ether (6 mL) at −78 °C with stirring. The mixture was allowed to warm to room temperature and stirred overnight. Evaporation of the solvent in vacuo yielded a crude product. To the crude product, dried CH_2Cl_2 (30 mL) was added, and the mixture was stirred for 10 min and filtered. The filtrate was evaporated in vacuo to afford a solid residue. To the solid residue, dried CH_2Cl_2 (3.0 mL) and dried *n*-hexane (20 mL) were added, and the mixture was stirred for 10 min. Filtration gave **5** (0.39 g, 0.69 mmol) as a dark purple solid in 36% yield; mp >300 °C. ^1H NMR($CDCl_3$): δ 6.01 (m, 2H, indole ring aromatic H), 6.7−7.3 (m, 4H, indole ring aromatic H + 10H, benzene ring aromatic H), 7.55 (m, 2H, indole ring aromatic H), 8.24 (s, 2H, CH═N), 8.35 (m, 2H, indole ring aromatic H). ^{13}C NMR data for complex **5** were not available since complex **5** was unstable in solution and thus decomposed during the ^{13}C NMR measurement. $C_{30}H_{22}N_4Cl_2Ti$: Calcd: C, 64.66; H, 3.98; N, 10.05. Found: C, 64.18; H, 4.10; N, 10.21. FD-MS (*m*/*z*) 556 (M^+).

[7-(2,3,4,5,6-F(Ph)NCH)$C_8H_5N]_2TiCl_2$ (8). To a stirred solution of **4** (1.00 g, 3.22 mmol) in dried toluene (30 mL) at 0 °C, a 1.56 M *n*-butyllithium hexane solution (2.17 mL, 3.38 mmol) was added dropwise over a 5 min period. The mixture was allowed to warm to room temperature and stirred for 4 h. The resulting mixture was added dropwise over a 20 min period to a 0.5 M *n*-heptane solution of $TiCl_4$ (3.22 mL, 1.61 mmol) in dried toluene (15 mL) at −78 °C with stirring. The mixture was allowed to warm to room temperature and stirred overnight. Evaporation of the solvent in vacuo yielded a crude product. To the crude product, dried CH_2Cl_2 (20 mL) was added, and the mixture was stirred for 10 min and filtered. The solid residue was washed with dried CH_2Cl_2 (20 mL × 3), and the combined organic filtrates were concentrated in vacuo to afford a dark purple solid. The solid was recrystallized from a dried CH_2Cl_2/dried *n*-hexane (1/1) solution (20 mL) at room temperature to give **8** (0.56 g, 0.76 mmol) as dark purple crystals in 47% yield; mp >300 °C. ^1H NMR($CDCl_3$): δ 6.21 (d, 2H, $J = 3.2$ Hz, indole ring aromatic H), 7.18−7.25 (m, 2H, indole ring aromatic H), 7.40 (d, 2H, $J = 7.0$ Hz, indole ring aromatic H), 7.84 (d, 2H, $J = 6.8$ Hz, indole ring aromatic H), 8.22 (d, 2H, $J = 2.7$ Hz, indole ring aromatic H), 8.32 (s, 2H, CH═N). ^{13}C NMR (100 MHz, $CDCl_3$): 104.2, 118.9, 122.2, 125−129, 128.9, 130.4, 131.3, 136−142, 139.8, 145.3, 173.2; $C_{30}H_{12}N_4F_{10}Cl_2Ti$ 737.20: Calcd: C, 48.88; H, 1.64; N, 7.60. Found: C, 48.40; H, 1.73; N, 7.72. FD-MS (*m*/*z*) 737 (M^+).

[7-(2,6-F(Ph)NCH)$C_8H_5N]_2TiCl_2$(6). 6 was prepared using a procedure similar to that for **8**; mp >300 °C. ^1H NMR($CDCl_3$): δ 5.98 (d, 2H, $J = 3.24$ Hz, indole ring aromatic H), 6.14 (m, 2H, benzene ring aromatic H), 6.73−6.78 (m, 4H, benzene ring aromatic H), 7.10 (t, 2H, $J = 7.6$ Hz, indole ring aromatic H), 7.31 (d, 2H, $J = 5.4$ Hz, indole ring aromatic H), 7.66 (dd, 2H, indole ring aromatic H), 8.19 (dd, 2H, indole ring aromatic H), 8.31 (s, 2H, N═CH). ^{13}C NMR (100 MHz, $CDCl_3$): 103.6, 110.4−112.0, 116.9, 119.3, 121.4, 125−127, 128.7, 128.9, 130.1, 140.0, 145.5, 153.5−156.0, 172.2. $C_{30}H_{18}N_4F_4Cl_2Ti$: Calcd: C, 57.26; H, 2.88; N, 8.90. Found: C, 56.56; H, 3.20; N, 9.12. FD-MS (*m*/*z*) 628 (M^+).

[7-(2,4,6-F(Ph)NCH)$C_8H_5N]_2TiCl_2$(7). 7 was prepared using a procedure similar to that for **8**; mp >300 °C. ^1H NMR($CDCl_3$): δ 5.85−5.95 (m, 2H, benzene ring aromatic H), 6.10 (d, 2H, $J = 3.2$ Hz, indole ring aromatic H), 6.49−6.55 (m, 2H, benzene ring aromatic H), 7.14 (t, 2H, $J = 7.6$ Hz, indole ring aromatic H), 7.33 (dd, 2H, indole ring aromatic H), 7.73 (dd, 2H, indole ring aromatic H), 8.20 (dd, 2H, indole ring aromatic H), 8.29 (s, 2H, N═CH). ^{13}C NMR (100 MHz, $CDCl_3$): 98.9−99.1, 99.6−100.9, 103.8, 119.2, 128.0−13.6, 128.6, 129.6, 139.8, 145.4, 153.5−160.8, 172.6. $C_{30}H_{16}N_4F_6Cl_2Ti$: Calcd: C, 54.17; H, 2.42; N, 8.42. Found: C, 54.15; H, 2.09; N, 8.23. FD-MS (*m*/*z*) 664 (M^+).

DFT Calculations.[35] All calculations were performed at the gradient corrected density functional BLYP level by means of the Amsterdam Density Functional (ADF 2001.01) program. We used the triple-ξ STO basis set for the titanium and the double-ξ STO basis set for the N, O, and methyl as a model of a polymer chain and the single-ξ STO basis set on the other atoms to calculate the optimized geometries. For energy calculations, the triple-ξ STO basis set for the titanium and the double-ξ plus polarization STO basis set for the other atoms were used, and the quasi-relativistic correction was also added.

Ethylene Polymerization. Ethylene polymerization was carried out under atmospheric pressure in toluene using a 500 mL glass reactor equipped with a mechanical stirrer, a temperature probe, and a condensor. Toluene (250 mL) was introduced to the nitrogen-purged reactor and stirred vigorously (600 rpm). The toluene was kept at a prescribed polymerization temperature, and then the ethylene gas feed (100 L/h) was started. After 15 min, polymerization was initiated by the addition of a toluene solution of MAO and then a toluene solution of a complex into the reactor with vigorous stirring (600 rpm). After a prescribed time, isobutyl alcohol (10 mL) was added to terminate the polymerization, and the ethylene gas feed was stopped. The resulting mixture was added to the acidic methanol (1 L including 2 mL of concentrated HCl). The solid polyethylene was recovered by filtration, washed with methanol (200 mL × 2), and dried (vacuum oven at 80 °C, overnight).

Preparation of a PE-*b*-poly(ethylene-*co*-propylene) Block Copolymer. To a nitrogen-purged 500 mL glass reactor equipped with a mechanical stirrer, a temperature probe, and a condensor, toluene (250 mL) was introduced and stirred vigorously (600 rpm). The toluene was kept at 2 °C using an ice-cold water bath, and then the ethylene gas feed (100 L/h) was started. After 15 min, polymerization was initiated by the addition of a 1.25 M toluene solution of MAO (2.0 mL, 2.5 mmol) and then a 0.002 M toluene solution of complex 7 (5.0 mL, 0.01 mmol) into the reactor with vigorous stirring (600 rpm). After 5 min, the feed gas was changed from ethylene to ethylene/propylene (30/70 L/h). After 50 min, the polymerization was terminated by the addition of isobutyl alcohol (10 mL). The resulting mixture was added to the acidic methanol (1000 mL including 2 mL of concentrated HCl). The polymer was collected by filtration, washed with methanol (200 mL × 2), and dried (vacuum oven at 120 °C, overnight).

Preparation of PE/poly(ethylene-*co*-propylene) Blend Sample for TEM Measurement. Polyethylene (200 mg, Table 4, entry 2) and ethylene/propylene copolymer (920 mg, Table 4, entry 3) and toluene (40 mL) were introduced to a nitrogen-purged 200 cm^3 reactor, and the contents were magnetically stirred for 5 min under nitrogen at room temperature. The mixture was heated at reflux temperature for 1 h with stirring. The resulting solution was poured into methanol (500 mL) at 60 °C. The precipitated polymer was collected by filtration, washed with methanol (200 mL × 2), and dried (vacuum oven at 80 °C, overnight).

TEM Analysis. Ultrathin (ca. 100 nm) sections of the polymers that had been pressed to give sheets and dyed with RuO_4 were prepared with a Reica Ultracut microtome equipped with a diamond knife at −100 °C. The specimens were examined with a Hitachi H-8100 transmission electron microscopy operating at 100 kV.

Acknowledgment. We thank Dr. M. Mullins for his fruitful discussions and suggestions. We also thank Y. Suzuki, Y. Yoshida, M. Mitani, J. Saito, H. Makio, S. Matsuo, H. Kaneko, Y. Tohi, Y. Nakayama, S. Matsuura, J. Mohri, S. Ishii, K. Tsuru, N. Matsukawa, Y. Sonobe, R. Furuyama, H. Bando, H. Terao, and J. S. Harp for their research and technical assistance.

Supporting Information Available: Calculated structures of ethylene coordinated active species, plot of polymer yield as a function of polymerization time, plot of M_n and M_w/M_n as a function of polymer yield, DSC measurements of PE and PF-*b*-poly(ethylene-*co*-propylene), and tables of ethylene polymerization results with complex/MAO catalyst systems. This material is available free of charge via the Internet at http://pubs.acs.org.

References and Notes

(1) For a review: Brinzinger, H. H.; Fischer, D.; Mülhaupt, R.; Rieger, B.; Waymouth, R. M. *Angew. Chem., Int. Ed. Engl.* **1995**, *34*, 1143.
(2) For reviews: (a) Biritovsek, G. J. P.; Gibson, V. C.; Wass, D. F. *Angew. Chem., Int. Ed.* **1999**, *38*, 428. (b) Ittel, S. D.; Johnson, L. K.; Brookhart, M. *Chem. Rev.* **2000**, *100*, 1169.
(3) Jeske, G.; Lauke, H.; Mauermann, H.; Swepston, P. N.; Schumann, H.; Marks, T. J. *J. Am. Chem. Soc.* **1985**, *107*, 8091.
(4) Yasuda, H.; Furo, M.; Yamamoto, H.; Nakamura, A.; Miyake, S.; Kibino, N. *Macromolecules* **1992**, *25*, 5115.
(5) Mashima, K.; Fujikawa, S.; Tanaka, Y.; Urata, H.; Oshiki, T.; Tanaka, E.; Nakamura, A. *Organometallics* **1995**, *14*, 2633.
(6) Hagihara, H.; Shiono, T.; Ikeda, T. *Macromolecules* **1998**, *31*, 3184.
(7) Fukui, Y.; Murata, M.; Soga, K. *Macromol. Rapid Commun.* **1998,** *20*, 637.

(8) Jayaratne, K. C.; Sita, L. R. *J. Am. Chem. Soc.* **2000**, *122,* 958. (b) Jayaratne, K. C.; Keaton, R. J.; Henningsen, D. A.; Sita, L. R. *J. Am. Chem. Soc.* **2000**, *122,* 10490. (c) Keaton, R. J.; Jayaratne, K. C.; Fettinger, J. C.; Sita, L. R. *J. Am. Chem. Soc.* **2000**, *122,* 12909.

(9) Hasan, T.; Ioku, A.; Nishii, K.; Shiono, T.; Ikeda, T. *Macromolecules* **2001**, *34*, 3142.

(10) Johnson, L. K.; Killian, C. M.; Brookhart, M. S. *J. Am. Chem. Soc.* **1995**, *117*, 6414. (b) Johnson, L. K.; Mecking, S.; Brookhart, M. *J. Am. Chem. Soc.* **1996**, *118*, 267. (c) Killian, C. M.; Tempel, D. J.; Johnson, L. K.; Brookhart, M. *J. Am. Chem. Soc.* **1996**, *118*, 11664. (d) Gates, D. P.; Svejda, S. A.; Onate, E.; Killian, C. M.; Johnson, L. K.; White, P. S.; Brookhart, M. *Macromolecules* **2000**, *33*, 2320.

(11) Wang, C.; Friedrich, A.; Younkin, T. R.; Li, R. T.; Grubbs, R. H.; Bansleben, A.; Day, M. W. *Organometallics* **1998**, *17*, 3149. (b) Younkin, T. R.; Connor, E. F.; Henderson, J. I.; Friedrich, S. K.; Grubbs, R. H.; Bansleben, D. A. *Science* **2000**, *287*, 460.

(12) Small, B. L.; Brookhart, M. S.; Bennett, A. A. *J. Am. Chem. Soc.* **1998**, *120*, 4049. (b) Britovsek, G. J. P.; Bruce, M.; Gibson, V. C.; Kimberley, B. S.; Maddox, P. J.; Mastroianni, S.; McTavish, S. J.; Redshaw, C.; Solan, G. A.; Strömberg, S.; White, A. J. P.; Williams, D. J. *J. Am. Chem. Soc.* **1999**, *121*, 8728.

(13) Hicks, F. A.; Brookhart, M. *Organometallics* **2001**, *20*, 3217.

(14) Scollard, J. D.; McConville, D. H.; Payne, N. C.; Vittal, J. J. *Macromolecules* **1996**, *29*, 5241. (b) Scollard, J. D.; McConville, D. H. *J. Am. Chem. Soc.* **1996**, *118*, 10008.

(15) Baumann, R.; Davis, W. M.; Schrock, R. R. *J. Am. Chem. Soc.* **1997**, *119*, 3830. (b) Baumann, R.; Schrock, R. R. *J. Organomet. Chem.* **1998**, *557*, 69. (c) Schrock, R. R.; Casado, A. L.; Goodman, J. T.; Liang, L.-C.; Bonitatebus, P. J., Jr.; Schrodi, *Organometallics* **2000**, *19*, 5325. (d) Schrock, R. R.; Bonitatebus, P. J., Jr.; Davis, M. W. *Organometallics* **2001**, *20*, 1056. (e) Mehrkhodavandi, P.; Bonitatebus, P. J., Jr.; Schrock, R. R. *J. Am. Chem. Soc.* **2000**, *122*, 12909.

(16) Stephan, D. W.; Guerin, F.; Spence, R. E. V. H.; Koch, L.; Gao, X.; Brown, S. J.; Swabey, J. W.; Wang, Q.; Xu, W.; Zoricak, P.; Harrison, D. G.; *Organometallics* **1999**, *18*, 2046.

(17) Gibson, V. C.; Maddox, P. J.; Newton, C.; Redshaw, C.; Solan, G. A.; White, A. J. P.; Williams, D. J. *Chem. Commun.* **1998**, 1651. (b) Matsuo, Y.; Mashima, K.; Tani, K. *Chem. Lett.* **2000**, 1114.

(18) (a) Murtuza, S.; Casagrande, O. L., Jr.; Jordan, R. F. *Polym. Mater. Sci. Eng.* **2001**, *84*, 109. (b) Michiue, K.; Murtuza, S.; Jordan, R. F. *Polym. Mater. Sci. Eng.* **2002**, *86*, 295.

(19) Tshuva, E. Y.; Goldberg, I.; Kol, M.; Weitman, H.; Goldschmidt, Z. *Chem. Commun.* **1997**, *18*, 635. (b) Tshuva, E. Y.; Goldberg, I.; Kol, M. *J. Am. Chem. Soc.* **2000**, *122*, 10706.

(20) Hakala, K.; Löfgren, B. Polamo, M.; Leskelä, M. *Macromol. Rapid Commun.* **1997**, *18*, 635.

(21) Doi, Y.; Ueki, S.; Keii, T. *Macromolecules* **1979**, *12*, 814.

(22) Mohring, V. M.; Fink, G. *Angew. Chem.* **1985**, *97*, 982; *Angew. Chem., Int. Ed. Engl.* **1985**, *24*, 1001.

(23) Brookhart, M.; DeSimone, J. M.; Grant, B. E.; Tanner, M. J. *Macromolecules* **1995**, *28*, 5378.

(24) Jeon, Y. M.; Park, S. J.; Heo, J.; Kim, K. *Organometallics* **1998**, *17*, 3161.

(25) Gottfried, A. C.; Brookhart, M. *Macromolecules* **2001**, *34*, 1140.

(26) Pioneering work concerning this field: (a) Bei, X.; Swenson, D. C.; Jordan, R. F. *Organometallics* **1997**, *16*, 3282. (b) Tsukahara, T.; Swenson, D. C.; Jordan, R. F. *Organometallics* **1997**, *16*, 3303. (c) Kim, I.; Nishihara, Y.; Jordan, R. F.; Rogers, R. D.; Rheingold, A. L.; Yap, P. A. *Organometallics* **1997**, *16*, 3314. (d) Jones, D.; Roberts, A. Cavell, K.; Keim, W.; Englert, U.; Skelton, B. W.; White, A. H. *J. Chem. Soc., Dalton Trans.* **1998**, 255. (e) Cozzi, P. G.; Gallo, E.; Floriani, C.; Chiesi-Villa, A.; Rizzoli, C. *Organometallics* **1995**, *14*, 4994.

(27) (a) Fujita, T.; Tohi, Y.; Mitani, M.; Matsui, S.; Saito, J.; Nitabaru, M.; Sugi, K.; Makio, H.; Tsutsui, T. **1998**, *EP-0874005*. (b) Mitani, M.; Yoshida, Y.; Mohri, J.; Tsuru, K.; Ishii, S.; Kojoh, S.; Matsugi, T.; Saito, J.; Matsukawa, N.; Matsui, S.; Nakano, T.; Tanaka, H.; Kashiwa, N.; Fujita, T. WO 01/55231 A1 2001; *Chem. Abstr.* **2001**, *135*, 137852. (c) Matsui, S.; Tohi, Y.; Mitani, M.; Saito, J.; Makio, H.; Tanaka, H.; Nitabaru, M.; Nakano, T.; Fujita, T. *Chem. Lett.* **1999**, 1065. (d) Saito, J.; Mitani, M.; Matsui, S.; Kashiwa, N.; Fujita, T. *Macromol. Rapid Commun.* **2000**, *21*, 1333. (e) Matsui, S.; Fujita, T. *Catal. Today* **2001**, *66*, 63. (f) Matsui, S.; Mitani, M.; Saito, J.; Tohi, Y.; Makio, H.; Matsukawa, N.; Takagi, Y.; Tsuru, K.; Nitabaru, M.; Nakano, T.; Tanaka, H.; Kashiwa, N.; Fujita, T. *J. Am. Chem. Soc.* **2001**, *123*, 6847. (g) Matsukawa, N.; Matsui, S.; Mitani, M.; Saito, J.; Tsuru, K.; Kashiwa, N.; Fujita, T. *J. Mol. Catal. A* **2001**, *169*, 99. (h) Saito, J.; Mitani, M.; Yoshida, Y.; Matsui, S.; Mohri, J.; Ishii, S.; Kojoh, S.; Kashiwa, N.; Fujita, T. *Angew. Chem., Int. Ed.* **2001**, *40*, 2918. (i) Kojoh, S.; Matsugi, T.; Saito, J.; Mitani, M.; Fujita, T.; Kashiwa, N. *Chem. Lett.* **2001**, 822. (j) Saito, J.; Mitani, M.; Onda, M.; Mohri, J.; Ishii, S.; Yoshida, Y.; Nakano, T.; Tanaka, H.; Matsugi, T.; Kojoh, S.; Kashiwa, N.; Fujita, T. *Macromol. Rapid Commun.* **2001**, *22*, 1072. (k) Ishii, S.; Saito, J.; Mitani, M.; Mohri, J.; Matsukawa, N.; Tohi, Y.; Matsui, S.; Kashiwa, N.; Fujita, T. *J. Mol. Catal. A* **2002**, *179*, 11. (l) Mitani, M.; Mohri, J.; Yoshida, Y.; Saito, J.; Ishii, S.; Tsuru, K.; Matsui, S.; Furuyama, R.; Nakano, T.; Tanaka, H.; Kojoh, S.; Matsugi, T.; Kashiwa, N.; Fujita, T. *J. Am. Chem. Soc.* **2002**, *124*, 3327. (m) Suzuki, Y.; Kashiwa, N.; Fujita, T. *Chem. Lett.* **2002**, 358. (n) Mitani, M.; Furuyama, R.; Mohri, J.; Saito, J.; Ishii, S.; Terao, H.; Kashiwa, N.; Fujita, T. *J. Am. Chem. Soc.*, in press. (o) Makio, H.; Kashiwa, N.; Fujita, T. *Adv. Synth. Catal.*, in press.

(28) Recently, group 4 transition metal complexes with phenoxy−imine ligands, named FI Catalysts, have been actively studied because of their high potential for olefin polymerization. For example: (a) Woodman, P. R.; Munslow, I. J.; Hitchcock, P. B.; Scott, P. K. *J. Chem. Soc., Dalton Trans.* **1999**, *22*, 4069. (b) Strauch, J.; Warren, T. H.; Erker, G.; Frohlich, R.; Saarenketo, P. *Inorg. Chim. Acta* **2000**, *300−302*, 810. (c) Killian, C. M. *MetCon 2000,* Proceedings, 2000. (d) Gibson, V. C.; Mastroianni, S.; Newton, C.; Redshaw, C.; Solan, G. A.; White, A. J. P.; Williams, D. J. *J. Chem. Soc., Dalton Trans.* **2000**, 1969. (e) Mackenzie, P. B.; Moody, L. S.; Killian, C. M.; Ponasik, J. A.; Lavoie, G. G.; Pearson, J. C.; Smith, T. W.; Tucker, L. A.; Moore, M.; Farthing, A.; King, G.; Meadows, M.; Sass, C.; Savitiski, E. *Proc. Am. Chem. Soc., Div. Polym. Mater.: Sci. Eng.* **2001**, *84*, 326. (f) Tian, J.; Hustad, P. D.; Coates, G. W. *J. Am. Chem. Soc.* **2001**, *21*, 5134. (g) Lamberti, M.; Pappalardo, D.; Zambelli, A.; Pellecchia, C. *Macromolecules* **2002**, *35*, 658. (h) Emslie, D. J. H.; Piers, W. E.; MacDonald, R. *J. Chem. Soc., Dalton Trans.* **2002**, 293. (i) Knight, P. D.; Clarke, A. J.; Kimberley, B. S.; Jackson, R. A.; Scott, P. *Chem. Commun.* **2002**, 352. (j) Hustad, P. D.; Tian, J.; Coates, G. W. *J. Am. Chem. Soc.* **2002**, *124*, 3614.

(29) Yoshida, Y.; Matsui, S.; Takagi, Y.; Mitani, M.; Nitabaru, M.; Nakano, T.; Tanaka, H.; Fujita, T. *Chem. Lett.* **2000**, 1270. (b) Yoshida, Y.; Matsui, S.; Takagi, Y.; Mitani, M.; Nakano, T.; Tanaka, H.; Kashiwa, N.; Fujita, T. *Organometallics* **2001**, *20*, 4793. (c) Yoshida, Y.; Saito, J.; Mitani, M.; Takagi, Y.; Matsui, S.; Ishii, S.; Nakano, T.; Kashiwa, N.; Fujita, T. *Chem. Commun.*, in press.

(30) Inoue, Y.; Nakano, T.; Tanaka, H.; Kashiwa, N.; Fujita, T. *Chem. Lett.* **2001**, 1060.

(31) Matsugi, T.; Matsui, S.; Kojoh, S.; Takagi, Y.; Inoue, Y.; Fujita, T.; Kashiwa, N. *Chem. Lett.* **2001**, 566.

(32) Dobson, D. R.; Gilmore, J.; Long, D. A. *Synlett* **1992**, 79. (b) Bartoli, G.; Palmieri, G. *Tetrahedron Lett.* **1989**, *30*, 2129.

(33) Piccolrovazzi, N.; Pino, P.; Consiglio, G.; Sironi, A.; Moret, M. *Organometallics* **1990**, *9*, 3098.

(34) Lee, L.; Gauthier, W. J.; Ball, J. M.; Iyengar, B.; Collins, S. *Organometallics* **1992**, *11*, 2115.

(35) (a) Guerra, C. F.; Snijders, J. G.; te Velde, G.; Baerends, E. J. *Theor. Chim. Acta* **1998**, *99*, 391. (b) te Velde, G.; Bickelhaupt, F. M.; van Gisbergen, S. J. A.; Fonseca Guerra, C.; Baerends, E. J.; Snijders, J. G.; Ziegler, T. *J. Comput. Chem.* **2001**, *22*, 931.

MA0122268